

Iterative Parameter Estimation for Metz Filter, Based on the Image Quality of Breast Cancer Imaging

Wira Hidayat Mohd Saad, *Member, IAENG*, Mohd Adzir Mahdi, Elias Saion, Suhairul Hashim, and M Iqbal Saripan, *Member, IAENG*.

Abstract—The main objective of the study is to estimate the iterative coefficient of Metz filter equation based on different point spread functions and its full width half maximum to acquire the best filtered image of semi-compressed breast phantom. The semi-compressed breast phantom image is generated using Monte Carlo N-Particle software version 5. Two parameters of the image quality, which are contrast to background ratio and fluctuation error are becoming our interest to be improved. These parameters indicate the visibility of the tumor and the presence of the noise in the image respectively. Every image is filtered with incremental value of the Metz filter iterative coefficient and full width half maximum of four different types of point spread function which are Gaussian, radial, Gaussian-ellipse and sinusoidal distortion. Varying these parameters will directly effect the tumor contrast and the fluctuation error of the image produced. The best filtered image produced is automatically selected, based on the output image with the highest tumor contrast and lowest fluctuation error. The algorithm is tested for one thousand samples of semi-compressed breast phantom image, to evaluate the performance of each different types of PSF and its relation to the selection of the iterative coefficient. At the end of the study, we propose an equation to estimate the iterative coefficient of Metz filter equation based on the suitable full width half maximum of Gaussian point spread function.

Index Terms—fluctuation error, contrast to background-ratio, Metz filter, point spread function

I. INTRODUCTION

STUDIES shows that the type of filter use with the imaging modalities can effect on the diagnosis of tumor detectability [1]–[4]. For the same reason, Metz filter had been developed to enhance the quality of image produced from the nuclear medical imaging [5]. Metz filter is derived as in equation below:

$$M(u, v) = \frac{1 - (1 - (H(u, v))^2)^X}{H(u, v)} \quad (1)$$

where $H(u, v)$ is an imaging modulation transfer function and X is an iterative coefficient that use to controls the extent to which the inverse filter (denominator) is followed before the filter switches to noise suppression using low pass filter (numerator). Parameter X is also known as iterative coefficient of Metz filter.

Manuscript received September 14, 2011; revised March 4, 2012.

W.H.M. Saad, M.I. Saripan and M.A. Mahdi are with Department of Computer and Communication Systems, Faculty of Engineering, University Putra Malaysia, 43400 Serdang, Selangor, Malaysia. Corresponding email: iqbal@eng.upm.edu.my

E. Saion is with Department of Physics, Faculty of Science, Universiti Putra Malaysia, 43400 Serdang, Selangor, Malaysia.

S. Hashim is with Department of Physics, Universiti Teknologi Malaysia, 81310 Skudai, Johor

Several study has been done to demonstrate the application of Metz filter in nuclear medical imaging [6]–[11]. Some study suggested that Metz filter show the best result compared with other types of filter such as Butterworth, Hanning and Ramp filter to improve scintigraphy image [12], [13]. This could be achieved by using a suitable parameter of the Metz filter equation. King *et al.* [6] suggested that the iteration coefficient, X can be estimated base on photons count. He used a count dependent Metz filter application on Alderson liver phantom image by scaling the image to several different counts per pixel before applying the filter. He came up with a function of X estimation that minimized mean square error value of the filtered image. On the other study [7], he proposed the other method of estimating an iterative coefficient based on constrained least-squares criterion restoration value to minimize the normalized mean square error on several different phantom images.

Our study's objective is to improve the tumor contrast and reduce noise presence in the image background. To achieve that, we propose an iterative algorithm in order to select the best outcome for individual image. With a current technology of high speed computer, iterative method is becoming more valid and reliable [14]. We applied the algorithm with one thousand image samples to find the relationship between the image quality and Metz filter parameters.

The process is done in a frequency domain where the original image, $G(x, y)$ is first converted from the spatial domain using 2D Fast Fourier Transform (FFT) to the frequency domain, $G(u, v)$. The convolution between original image and Metz filter transfer function, $M(u, v)$ is done in a frequency domain as shown by equation below:

$$F(u, v) = M(u, v)G(u, v) \quad (2)$$

Subsequently, the filtered image, $F(u, v)$ is converted back to the spatial domain, $F(x, y)$ using inverse 2D-FFT to measure the image quality for display purposes.

II. GENERATING THE IMAGE SAMPLES

Semi-compressed breast phantom is constructed by using four simple geometry, consist of two rectangular polygons to represent the breast and torso, and two spheres to represent the heart and tumors. The torso and the heart are added to the breast phantom in order to simulate the scattering effect cause by the body part that located near the breast. The tumor was set to be 10 mm diameter and located at 3 cm depth from the breast surface. The heart is located inside the torso with 8 cm diameter. The rests of the dimensions are shown in Fig. 1.

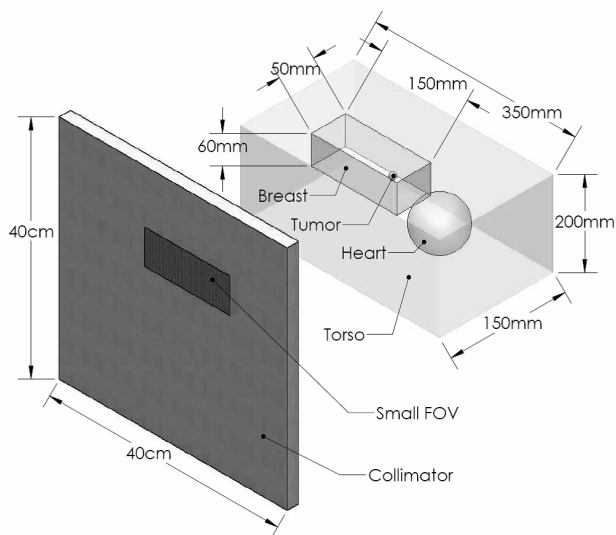


Fig. 1. Breast phantom and collimator dimension set up in MCNP5 simulation environment

This phantom application basically follow the work done by Gruber *et al.* [15]. In the study, they simulated the phantom with a discrete compact gamma camera. Alnafea *et al.* [16] also used the same phantom to test the modified uniformly-redundant array-coded aperture gamma camera.

In this study, we simulate the semi-compressed breast phantom using wire mesh collimator gamma camera [17]. We used Toshiba GCA 7100A gamma camera model as a reference configuration set up in MCNP5 [18], [19]. Previously, wire mesh collimator was configured to give an optimized performance when simulated with the semi-compressed breast phantom [20]. Even though wire mesh collimator had been optimized with semi-compressed breast phantom, the quality of the image produced is still not adequate, since image can be degraded by several factors, such as limited spatial resolution of gamma camera, Compton scattering, septa penetration and Poisson noise cause in radioactive decay process. By applying a Metz filter, poor image quality associated with the above problems will be improved [5]–[8], [10].

Semi-compressed breast phantom is positioned at 3 cm from the surface of the collimator. The dimension of the wire mesh collimator is 40 x 40 x 4.02 cm. We used rectangular type of Tungsten wire mesh with hole dimension of 0.15 x 0.15 cm, and septa thickness (wire diameter) is 0.02 cm. Sodium Iodide detector with density of 3.67 g/cm³ and dimension of 40 x 40 x 0.9525 cm is placed behind the collimator without any gap. The size of each pixel is set at 0.3125 x 0.3125 cm² and energy acceptance window is 126-154 keV. The pixel location for each of the photons deposition is determined using Anger logic algorithm. We only consider the dark region as shown in Fig. 1 to produce an image as this region covered breast and tumor area. The size of the image produced on this region is 13 x 45 pixels.

The composition of the breast phantom materials are uniformly distributed in each of the parts. The materials composition and density are referred to the ICRU report 44 [21].

Energy of the photons emission is set to be 140 keV. Activ-

ity density for breast and torso is assumed to be 80 nCi/cm³ and heart activity density is ten time greater then activity on the breast and torso which is 800 nCi/cm³. Tumor to the background ratio (TBR) is set to be 10:1. Approximately, $\sim 2.37 \times 10^{10}$ number of photons are simulated to impersonate 10 minutes of the imaging time. Each part of the phantom is simulated separately, and the final simulation result of each part is combined. To generate different variation of output images, breast and tumor are simulated several times with the different random number generator initialization (seed number).

III. EVALUATING THE IMAGE QUALITY

The quality of the image is measured using contrast to background ratio (CBR) and fluctuation error of the image on the breast area.

Tumor contrasts can be measured using CBR equation [16], [22], [23]. The CBR produce similar characteristic as signal to noise ratio (SNR) [20]. Since the CBR calculation cover more pixel area then SNR, using CBR instead of SNR will give more consistent evaluation for the semi-compressed breast phantom image. The CBR is represented by the following equation:

$$CBR = \frac{i_{tp} - \bar{i}_{mn}}{\bar{i}_{mn}} \quad (3)$$

where i_{tp} is the pixel value at the tumor peak and \bar{i}_{mn} is the average pixel value on the breast area.

Pixel value on the breast area is fluctuated even thought the material and photons emission is uniformly distributed. This is due to the presence of noise as the result of interaction of photons with matter. The equation of the fluctuation error is shown in following equation:

$$FE = \sqrt{\frac{1}{nm} \sum_x^n \sum_y^m (i(x,y) - \bar{i}_{mn})^2} \quad (4)$$

Equation 4 is applied on the selected region with the pixel size of $m \times n$, around breast area excluding the tumor area, $i(x,y)$ is a pixel value of (x,y) location. \bar{i}_{mn} is average pixel value on the selected region. In other words, fluctuation error is a standard deviation of the selected region on the breast area.

The histogram normalization is applied on the image before measuring CBR and fluctuation error, so that the calculation can be done to the image before it being displayed.

IV. METHODOLOGY

The PSF can be defined by the response of the ideal imaging system to an isotropic point source. Gamma camera with wire mesh collimator produced a Gaussian like distribution when simulated with a single isotropic point source [17], [20]. The FWHM of PSF is slightly changed when configuration of the internal layer of the wire mesh collimator is altered. The FWHM of the gamma camera PSF also can be affected by several factors such as distance of the point source to the collimator, septa thickness and hole size. To overcome this uncertainty, we generate a 2D Gaussian PSF from the equation, so that the value FWHM can be manipulated.

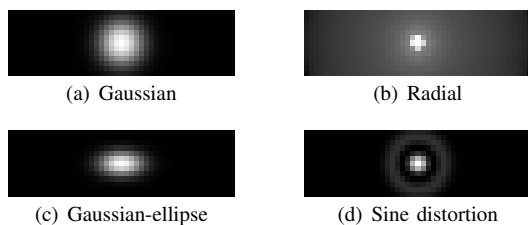


Fig. 2. Different types of PSF image generated in this study where $c=3$

Other than Gaussian PSF, we also generate another three different types of commonly used PSF which are radial, Gaussian-ellipse and sinusoidal distortion types [24], [25]. Here, we want to observe the effect of different PSFs to our proposed algorithm. Gaussian, Gaussian-ellipse and sinusoidal distortion transfer function are shown in Equation 5, 6 and 7 respectively.

$$h_g(x, y) = a \cdot \exp\left(-\frac{(x-x_o)^2 + (y-y_o)^2}{2c^2}\right) \quad (5)$$

$$h_{ge}(x, y) = a \cdot \exp\left(-\left(\frac{(x-x_o)^2}{2\left(\frac{M}{N}c\right)^2} + \frac{(y-y_o)^2}{2c^2}\right)\right) \quad (6)$$

$$h_s(x, y) = h_g(x, y) \cdot \frac{1}{2} \left(\cos\left(\frac{\pi}{c} \cdot \sqrt{(x-x_o)^2 + (y-y_o)^2}\right) + 1 \right) \quad (7)$$

Parameter a is set to be 255, as it is a maximum pixel value of the PSF image, x_o and y_o is center of the PSF image and c is a parameter that relates to FWHM of the PSF. By increasing this parameter, it will broaden the FWHM of the PSF. The size of the PSF image generated, $m \times n$ is equal to the size of the image to be processed which is 13×45 pixels.

Radial type of PSF is created by the arrangement of the pixel value from the original image, starting from the center pixel at $i(x_o, y_o)$ with highest pixel value to the pixel location that furthest from the center with lowest pixel value, based on the Euclidean distance [26]. Illustration of four different types of PSF images are shown in Fig. 2.

The algorithms of the proposed method are summarized by the flow diagram shown on Fig. 3. First, image produce by MCNP5 is normalized to 8 bit grayscale, in order to calculate the initial value of CBR and fluctuation error. Images will be processed using Metz filter equation with four different types of PSFs. For each type of different PSF applied, parameter X and c is varied in every iteration, and the value of CBR and fluctuation error is calculated on the output image after the output image is normalized to 8 bit grayscale. The value of CBR and fluctuation error are plotted for each iteration to estimate a point where both CBR and fluctuation error are on its highest value.

Fig. 4 is an example of the plot for CBR vs. X and fluctuation error vs. X of a particular image sample, before and after filtered using Metz equation with Gaussian-ellipse PSF ($c=1$). From the plot, it can be noted that the CBR of the output image is maximum when $X=1$ and fluctuation error is minimum when $X=1.2$. The algorithm will automatically select the value in between both of it which is at $X=1.1$. The characteristic of the CBR and fluctuation error plot are similar for different c parameters, the same algorithm is applied to all iteration. At this point, we will have several

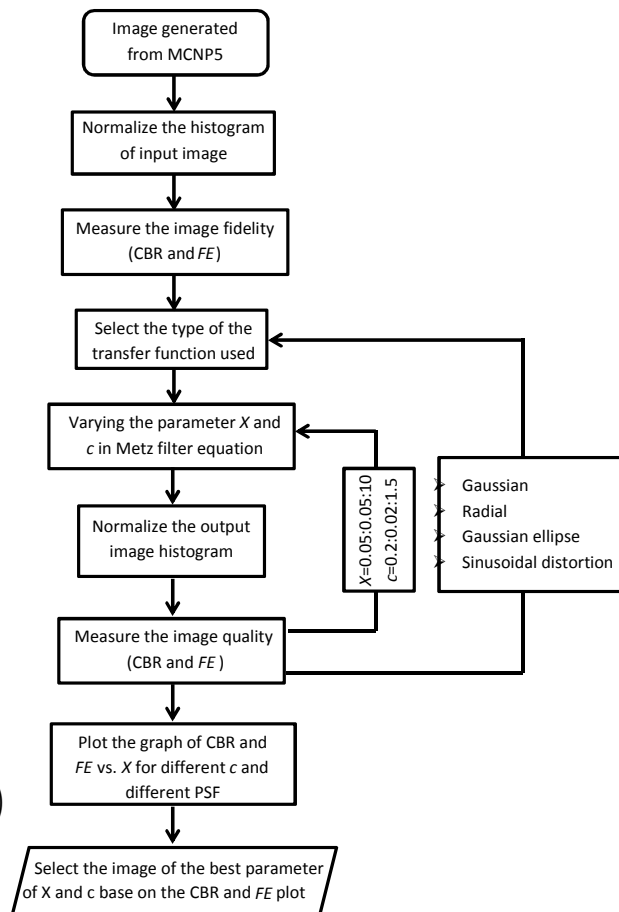


Fig. 3. Flow diagram of the image processing

filtered images for different c parameters used. Among these images, the algorithm will select the final image based on the best image quality displayed. The parameters of X and c that been used to generate this final image are recorded.

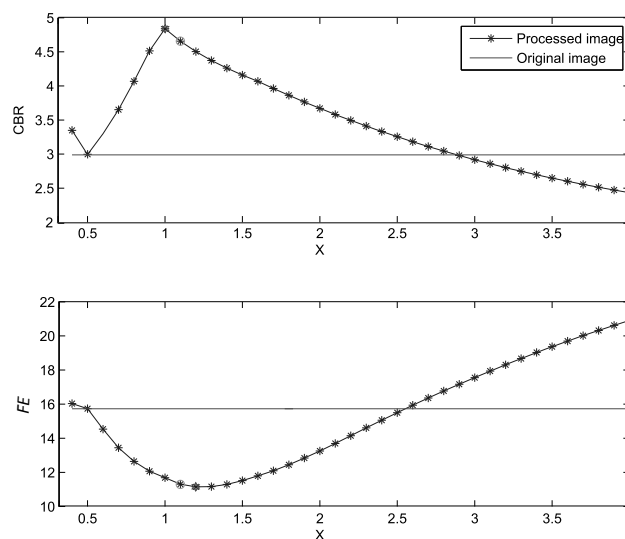


Fig. 4. Plot of Metz filter result; CBR vs. X and fluctuation error vs. X for one of the image sample, using Gaussian-ellipse PSF with $c=1$

V. RESULT AND DISCUSSION

One thousand of semi-compressed breast images were tested using the iterative algorithm described in Section IV. Fig. 6 is a plot of CBR against Fluctuation error for original image and processed image. It shows that, CBR is inversely proportionate to fluctuation error. We can conclude that, when the presence of the noise in the image of breast tumor is reduced, it will enhance the visibility of the tumor.

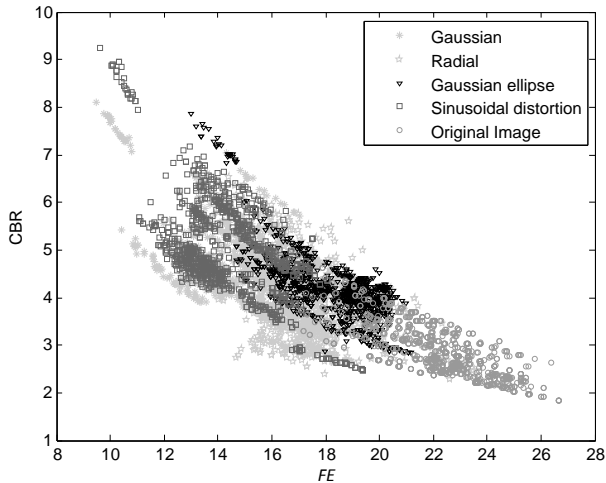


Fig. 5. Plot of the CBR vs. fluctuation error before and after process using four different type of PSF

The plot on Fig. 5 is summarized into a cumulative distribution plot as shown in Fig. 6 and 7. It shows that, using of sinusoidal distortion PSF give the output image quality as good as by using Gaussian PSF. The other two PSF are not encouraging enough compare to the Gaussian and sinusoidal distortion. Generally, every image samples shows at least a small improvement after the filtering process. This is because, the best quality image can possibly be selected by using the iterative algorithm.

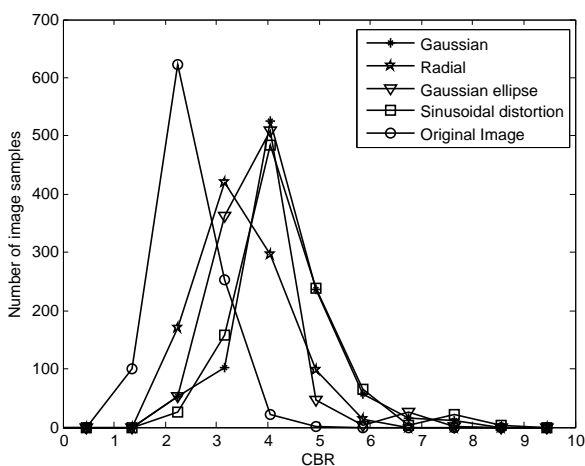


Fig. 6. Sample distribution of the CBR for the original image and image after processed. The mean, μ and standard deviation, σ of the distribution is written as $CBR(\mu, \sigma)$, starting for Gaussian PSF, $CBR_g(4.72, 0.87)$, Radial PSF, $CBR_r(3.92, 0.81)$, Gaussian-ellipse PSF, $CBR_{ge}(4.19, 0.70)$, sinusoidal distortion, $CBR_{sd}(4.73, 0.91)$ and original image, $CBR_{or}(2.86, 0.53)$

Table I shows two examples of original image samples and its filtered image, by using these four type of PSFs.

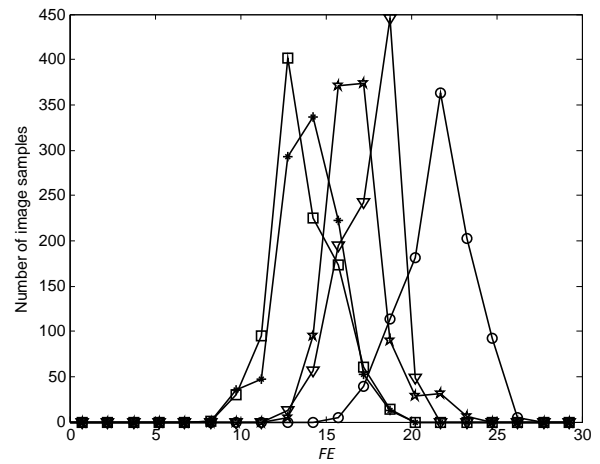


Fig. 7. Sample distribution of the fluctuation error for the original image and after filtered image. The mean, μ and standard deviation, σ of the distribution is written as $FE(\mu, \sigma)$, starting for Gaussian PSF, $FE_g(14.81, 1.69)$, Radial PSF, $FE_r(17.52, 1.64)$, Gaussian-ellipse PSF, $FE_{ge}(18.29, 1.59)$, sinusoidal distortion, $FE_{sd}(14.47, 1.78)$ and original image, $FE_{or}(22.26, 1.88)$

Visually, all the filtered images are less fluctuated compared to the original image. The image process using a Radial PSF appeared to be blurred and the tumor size seem to be enlarged from it original size. This is due to the fact that, only this type of PSF is not adjustable. Whereas, the image filtered using a Gaussian-ellipse PSF, tumor size seem to be expanded from it original size because this PSF is not isometric.

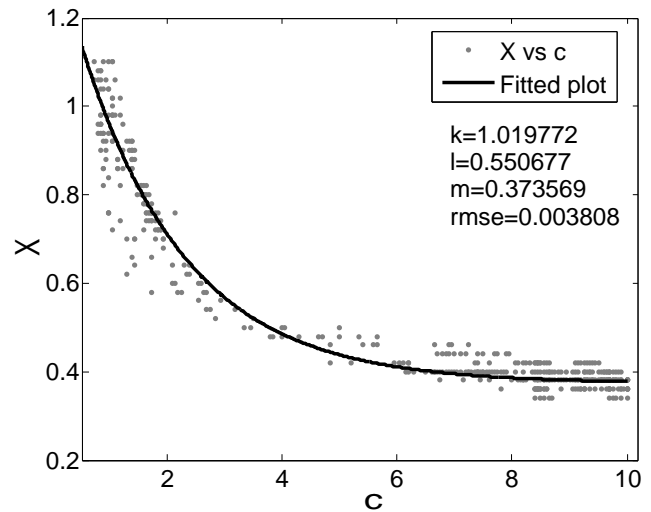


Fig. 8. Plot of parameter X versus parameter c of Gaussian PSF equation for one thousand simulated images of semi-compressed breast phantom, determined by optimizing the tumor contrast and the fluctuation error.

Fig. 8 shows the plot of X vs. c by using Gaussian PSF. The plot shows that, FWHM of the Gaussian PSF to the iterative coefficient is inverse exponential. However, it does not show the same relationship (Fig. 9), when we plot the same parameters for sinusoidal distortion even though both of this PSF shows a comparably good performance. As discussed earlier, gamma camera PSF is similar to the 2D Gaussian distribution function. That makes Gaussian PSF is the most suitable function to substitute the gamma camera PSF.

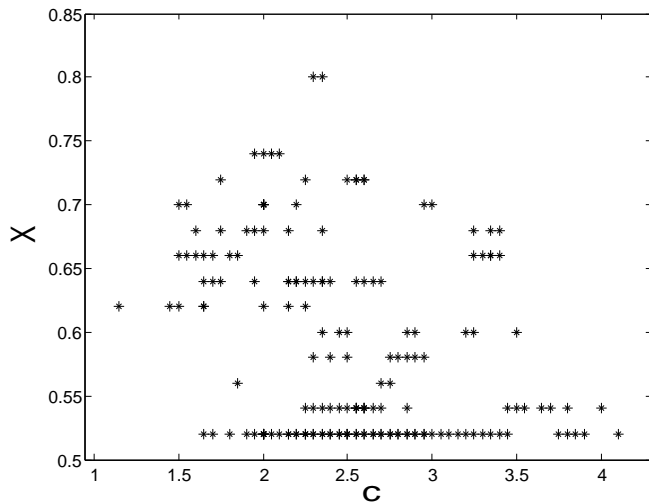


Fig. 9. Plot of parameter X versus parameter c of sinusoidal distortion PSF equation for one thousand simulated images of semi-compressed breast phantom, determined by optimizing the tumor contrast and the fluctuation error

The plot on Fig. 8 can be fitted by the following equation:

$$Exponential_{fitted} = k(e^{-lc}) + m \quad (8)$$

where k , l and m are the coefficient value of the best fit, based on 99% of confident interval using non-linear least square technique. Parameter c is related to FWHM of the Gaussian PSF and can be expressed by:

$$FWHM = 2.3548c \quad (9)$$

where FWHM is measured in the pixels. By replacing parameters k , l and m on Equation 8 to its fitted value, the relationship between iterative parameters of Metz filter equation, X and FWHM for the Gaussian PSF can be written as:

$$X = 1.019772.e^{-1.296745FWHM} + 0.373569 \quad (10)$$

To use this equation, we still need to have the value of FWHM for Gaussian PSF. This could be attained by applying the iterative algorithm as proposed by the above method. The time used to process each image will be reduced, since we only required to estimate value of one parameter only.

VI. CONCLUSION

In this study, we managed to demonstrate the iterative method in selecting the parameters used to apply Metz filter for semi-compressed breast simulation using wire mesh collimator gamma camera. The method is tested with one thousand images of semi-compressed breast phantom to evaluate the selection algorithm of the parameter estimation. We also compared the effect of using four different types of PSFs as modulation transfer function for the Metz filter equation. The results showed that, in addition to Gaussian PSF, sinusoidal distortion PSF also demonstrate a good performance with the majority image samples. Finally, we proposed the equation to estimate the value of the Metz filter iterative coefficient based on the FWHM of the Gaussian PSF.

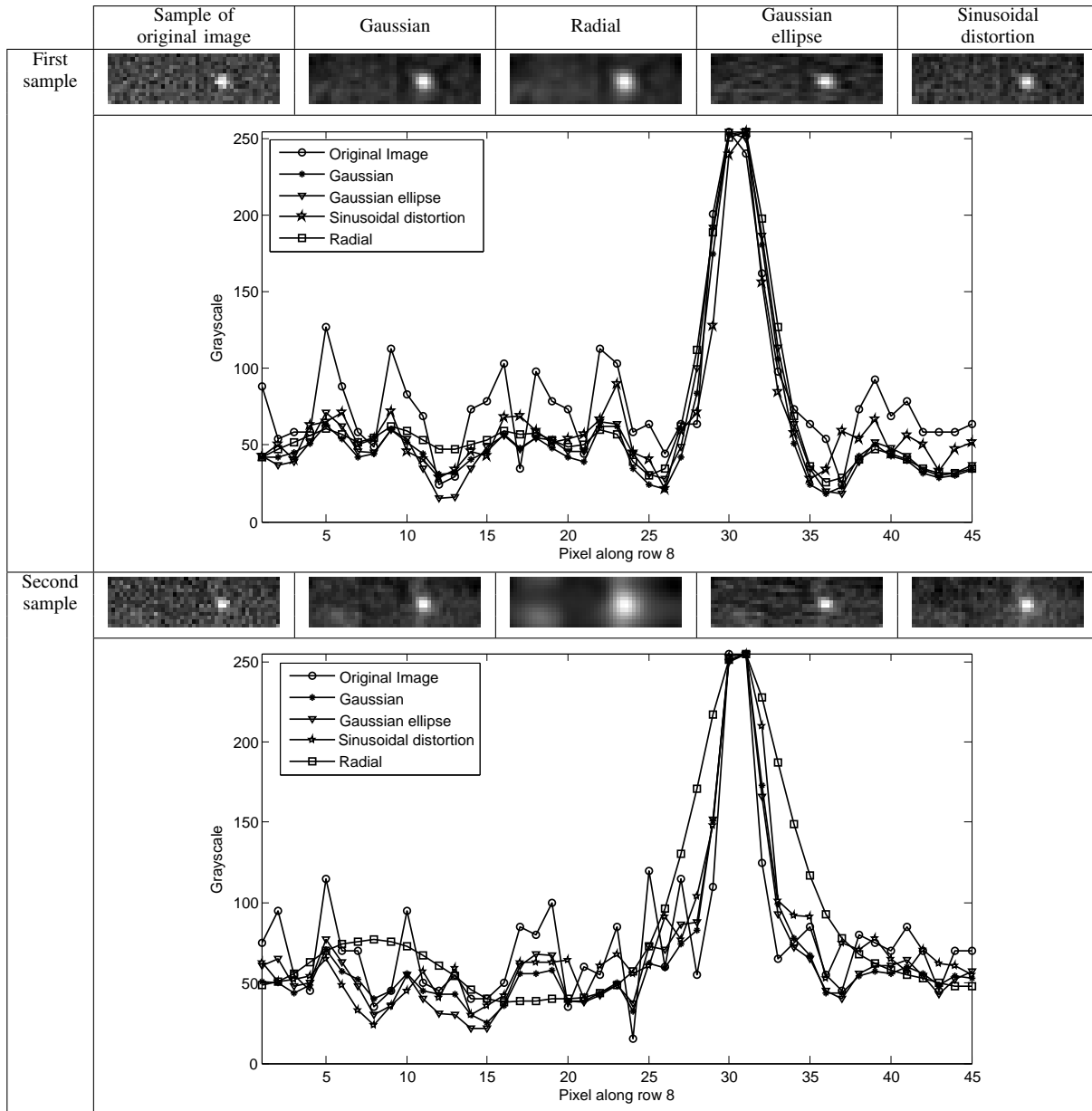
ACKNOWLEDGMENT

The authors would like to thank Universiti Putra Malaysia and Universiti Teknikal Melaka for the Fellowship assistant.

REFERENCES

- [1] P. F. Judy and R. G. Swenson, "Detection of small focal lesions in CT images: Effects of reconstruction filters and visual display windows," *British Journal of Radiology*, vol. 58, no. 686, pp. 137–145, 1985.
- [2] D. R. Gilland, B. M. W. Tsui, W. H. McCartney, J. R. Perry, and J. Berg, "Determination of the optimum filter function for SPECT imaging," *Journal of Nuclear Medicine*, vol. 29, no. 5, pp. 643–650, 1988.
- [3] S. Chucherd and S. S. Makhanov, "Sparse phase portrait analysis for preprocessing and segmentation of ultrasound images of breast cancer," *IAENG International Journal of Computer Science*, vol. 38, no. 2, pp. 146–159, 2011.
- [4] I. Avazpour, R. E. Roslan, P. Bayat, M. I. Saripan, A. J. Nordin, and R. S. A. R. Abdullah, "Segmenting ct images of bronchogenic carcinoma with bone metastases using PET intensity markers approach," *Radiology and Oncology*, vol. 43, no. 3, pp. 180–186, 2009.
- [5] C. E. Metz, "A mathematical investigation of radioisotope scan image processing," Ph.D. dissertation, University of Pennsylvania, January 1969.
- [6] M. A. King, R. B. Schwinger, P. W. Doherty, and B. C. Penney, "Two-dimensional filtering of SPECT images using the Metz and Wiener filters," *Journal of Nuclear Medicine*, vol. 25, no. 11, pp. 1234–1240, 1984.
- [7] M. A. King, B. C. Penney, and S. J. Glick, "An image-dependent Metz filter for nuclear medicine images," *Journal of Nuclear Medicine*, vol. 29, no. 12, pp. 1980–1989, 1988.
- [8] C. E. Metz and R. N. Beck, "Quantitative effects of stationary linear image processing on noise and resolution of structure in radionuclide images," *Journal of Nuclear Medicine*, vol. 5, no. 3, pp. 164–170, March 1974.
- [9] A. K. Pandey, G. S. Pant, and A. Malhotra, "Standardization of SPECT filter parameters," *Indian Journal of Nuclear Medicine*, vol. 19, no. 2, pp. 30–35, 2004.
- [10] J. Varga, V. Bettinardi, M. C. Gilardi, C. Riddell, I. Castiglioni, G. Rizzo, and F. Fazio, "Evaluation of pre- and post-reconstruction count-dependent Metz filters for brain PET studies," *Medical Physics*, vol. 24, no. 9, pp. 1431–1440, 1997.
- [11] J. S. Liow and S. C. Strother, "Noise and signal decoupling in maximum-likelihood reconstructions and Metz filters for PET brain images," *Physics in Medicine and Biology*, vol. 39, no. 4, pp. 735–750, 1994.
- [12] A. P. Pant and A. Malhotra, "Standardization of SPECT filter parameters," *International Journal of Nuclear Medicine*, vol. 19, no. 2, pp. 30–35, 2004.
- [13] M. Lyra and A. Ploussi, "Filtering in SPECT image reconstruction," *International Journal of Biomedical Imaging*, vol. 2011, 2011.
- [14] I. Goddard, T. Wu, S. Thieret, A. Berman, and H. Bartsch, "Implementing an iterative reconstruction algorithm for digital breast tomosynthesis on graphics processing hardware," in *Progress in Biomedical Optics and Imaging - Proceedings of SPIE*, vol. 6142 III, 2006.
- [15] G. J. Gruber, "Monte carlo simulations of breast tumor imaging properties with compact, discrete gamma cameras," *IEEE Transactions on Nuclear Science*, vol. 46, no. 6, pp. 2119–2123, 1999.
- [16] M. Alnafa, K. Wells, N. M. Spyrou, M. Saripan, M. Guy, and P. Hinton, "Preliminary results from a Monte Carlo study of breast tumor imaging with low-energy high-resolution collimator and a modified uniformly-redundant array-coded aperture," *Nuclear Instruments and Methods in Physics Research A*, vol. 563, pp. 146–149, 2006.
- [17] M. I. Saripan, M. Petrou, and K. Wells, "Wire mesh collimator gamma camera," *IEEE Transactions on Biomedical Engineering*, vol. 54, no. 9, pp. 1598–1612, Sep. 2007.
- [18] M. I. Saripan, K. Wells, M. Petrou, M. Alnafa, and M. Guy, "Design of a multihole collimator gamma camera model for use in Monte Carlo simulation," *Proceeding of the Medical Image Understanding and Analysis*, vol. 1, pp. 87–90, 2005.
- [19] M. I. Saripan, S. Hashim, S. Mashohor, W. A. W. Adnan, and M. H. Marhaban, "Characteristics of multihole collimator gamma camera simulation modeled using MCNP5," *AIP Conference Proceedings*, vol. 1017, pp. 205–209, 2008.
- [20] W. H. M. Saad, R. E. Roslan, M. A. Mahdi, W. S. Choong, E. Saion, and M. I. Saripan, "Monte Carlo design of optimal wire mesh collimator for breast tumor imaging process," *Nuclear Instruments and Methods in Physics Research Section A: Accelerators, Spectrometers, Detectors and Associated Equipment*, vol. 648, no. 1, pp. 254 – 260, 2011.

TABLE I
COMPARISON OF THE PROCESSED IMAGE USING FOUR DIFFERENT TYPE OF POINT SPREAD FUNCTION



[21] ICRU, "Tissue substitutes in radiation dosimetry and measurement," International Commission on Radiation Units and Measurements, Tech. Rep. 44, 1989.

[22] M. I. Saripan, W. H. M. Saad, M. A. Mahdi, and A. R. Ramli, "Research note: Early cancer detection with wire mesh collimator gamma camera," *International Review of Physics*, vol. 2, pp. 184–186, 2008.

[23] M. I. Saripan, W. H. M. Saad, S. Hashim, R. Mahmud, A. J. Nordin, and M. A. Mahdi, "Monte Carlo simulation on breast cancer detection using wire mesh collimator gamma camera," *IEEE Transactions on Nuclear Science*, vol. 56, no. 3, pp. 1321–1324, June 2009.

[24] C. Y. Wen and C. H. Lee, "Point spread functions and their applications to forensic image restoration," *Forensic Science Journal*, vol. 1, pp. 15–26, 2002.

[25] D. Li, R. M. Mersereau, and S. Simske, "Atmospheric turbulence-degraded image restoration using principal components analysis," *IEEE transaction of Geoscience and Remote Sensing Letters*, vol. 4, no. 3, pp. 340–344, July 2007.

[26] M. Saripan, N. Kamar, and A. Ramli, "Power spectra estimation using the combination of Goodman and Belsher method with a constant on gamma camera images," *IAENG International Journal of Computer Science*, vol. 36, no. 4, 2009.

Wira Hidayat Mohd Saad (M'11) received the B. Eng. degree in Electrical and Electronic Engineering from Universiti Putra Malaysia in 2007.

Currently he continues his study in Doctor of Philosophy program with field of study in Multimedia System Engineering at Universiti Putra Malaysia. His research interests are in the area of medical imaging.

Mr Mohd Saad is a member of the IEEE Engineering in Signal Processing Society.

Mohd Adzir Mahdi received Bachelor degree with first class honors in electrical, electronics and systems engineering from Universiti Kebangsaan Malaysia, Selangor, Malaysia in 1996. Later, he received the Master and Ph.D. degrees with distinctions in optical fiber communications from the Universiti Malaya, Kuala Lumpur, Malaysia in 1999 and 2002, respectively.

He joined the Faculty of Engineering, Universiti Putra Malaysia, Selangor, Malaysia in January 2003 and now he become a professor. He is now the Deputy Director of Knowledge Management Unit at Research Management Center and Research Fellow at the Photonics Transmission Cluster, TM Research & Development Sendirian Berhad.

Prior to the current appointment, Adzir was an optical design engineer at IOA Corporation, Sunnyvale, USA and a research officer at Research and Development Division, Telekom Malaysia Berhad. He was a visiting researcher at Marconi SpA in January and from June to July in 1998 and a visiting researcher at Monash University from April to May in 2007.

Since 1996, he had been involved in photonics research specializing in optical amplifiers and lasers. He had authored and coauthored over 110 journal papers and 130 conference papers. His research interest includes optical fiber amplifiers and lasers, optical fiber communications and nonlinear optics.

Dr. Mahdi is also a member of the Optical Society of America and the International Association of Engineers.

Elias Saion received the BSc. degree in Physics from National Universiti of Malaysia, in 1975 MSc degree in Medical Physics from Universiti of Surrey, United Kingdom in 1978 and PhD in Radiation Biophysics from University of St Andrews, United Kingdom, in 1989

He is now appointed as a Professor in Physics Department, Universiti Putra Malaysia and as a Joint Researcher in Institute for Mathematical Research, Universiti Putra Malaysia. His research interest is in applied radiation, polymer gel dosimeters for radiotherapy, electrical and optical properties of irradiated polymer blends, conducting polymers induced by ionizing radiation, ionic polymer electrolytes and Sulfonated organic or inorganic polymer/metal oxide nanocomposites for fuel cell applications.

He is a members of Mathematics Sciences Malaysia Associations since 2003 and members of Malaysian Cryptographic Research Society since 2005.

Suhairul Hashim Suhairul Hashim received his first degree in Nuclear Science from Universiti Kebangsaan Malaysia (UKM) in 2001. Upon graduation, he was employed by Universiti Teknologi Malaysia (UTM) and awarded a scholarship to pursue his study towards Master degree. He obtained Master of Science in Medical Physics from University of Surrey, U.K. in 2005.

He was granted the degree of Doctor of Philosophy (PhD) from Universiti Teknologi Malaysia in March 2009 with PhD thesis entitled The thermoluminescence response of doped silicon dioxide optical fibres to ionizing radiation. Then, he was awarded a postdoctoral fellowship funded by the University of Michigan, U.S to gain an experience as a research fellow at the University of Surrey, U.K.

Currently, he is a senior lecturer and a researcher in UTM. His current research interest is in Medical Radiation Physics and Dosimetry System.

M Iqbal Saripan (M'06) received his B.Eng. degree in Electronics Engineering from Universiti Teknologi Malaysia in 2001 and PhD. degree in Medical Imaging from University of Surrey, Guildford, U.K. in 2006. Currently, he is a Associate Professor at the Department of Computer and Communication Systems Engineering, Faculty of Engineering, Universiti Putra Malaysia. His research interests are in the area of medical imaging, speech processing, and embedded system.

Dr. Saripan is also a member of the IEEE and Institute of Physics UK